

# Correlation of Carotid Intraplaque Hemorrhage and Stroke Using 1.5 T and 3 T MRI

Supplement Issue: New Concepts in Magnetic Resonance as Applied to Cellular and In Vivo Applications

Gerald S. Treiman<sup>1-3</sup>, J. Scott McNally<sup>1</sup>, Seong-Eun Kim<sup>1</sup> and Dennis L. Parker<sup>1</sup>

<sup>1</sup>Utah Center for Advanced Imaging Research, Department of Radiology, University of Utah, Salt Lake City, Utah, USA. <sup>2</sup>Department of Surgery, VA Salt Lake City Health Care System, Salt Lake City, Utah, USA. <sup>3</sup>Department of Surgery, University of Utah, Salt Lake City, Utah, USA.

**ABSTRACT:** Carotid atherosclerotic disease causes approximately 25% of the nearly 690,000 ischemic strokes each year in the United States. Current risk stratification based on percent stenosis does not provide specific information on the actual risk of stroke for most individuals. Prospective randomized studies have found only 10 to 12% of asymptomatic patients will have a symptomatic stroke within 5 years. Measurements of percent stenosis do not determine plaque stability or composition. Reports have concluded that cerebral ischemic events associated with carotid plaque are intimately associated with plaque instability. Analysis of retrospective studies has found that plaque composition is important in risk stratification. Only MRI has the ability to identify and measure the detailed components and morphology of carotid plaque and provides more detailed information than other currently available techniques. MRI can accurately detect carotid hemorrhage, and MRI identified carotid hemorrhage correlates with acute stroke.

**KEYWORDS:** MRI, carotid, hemorrhage

**SUPPLEMENT:** New Concepts in Magnetic Resonance as Applied to Cellular and In Vivo Applications

**CITATION:** Treiman et al. Correlation of Carotid Intraplaque Hemorrhage and Stroke Using 1.5 T and 3 T MRI. *Magnetic Resonance Insights* 2015;8(S1) 1–8  
doi:10.4137/MRI.S23560.

**RECEIVED:** February 24, 2015. **RESUBMITTED:** April 6, 2015. **ACCEPTED FOR PUBLICATION:** April 13, 2015.

**ACADEMIC EDITOR:** Sendhil Velan, Editor in Chief

**TYPE:** Review

**FUNDING:** This work has been funded in part by a merit review grant from the Department of Veterans Affairs (11736847). The authors confirm that the funder had no influence over the study design, content of the article, or selection of this journal.

**COMPETING INTERESTS:** Authors disclose no potential conflicts of interest.

**COPYRIGHT:** © the authors, publisher and licensee Libertas Academica Limited. This is an open-access article distributed under the terms of the Creative Commons CC-BY-NC 3.0 License.

**CORRESPONDENCE:** gstreiman@earthlink.net

Paper subject to independent expert blind peer review by minimum of two reviewers. All editorial decisions made by independent academic editor. Upon submission manuscript was subject to anti-plagiarism scanning. Prior to publication all authors have given signed confirmation of agreement to article publication and compliance with all applicable ethical and legal requirements, including the accuracy of author and contributor information, disclosure of competing interests and funding sources, compliance with ethical requirements relating to human and animal study participants, and compliance with any copyright requirements of third parties. This journal is a member of the Committee on Publication Ethics (COPE).

Published by Libertas Academica. Learn more about this journal.

## Introduction

**Carotid atherosclerosis.** Atherosclerotic disease of the carotid artery is the direct cause of 173,000 or approximately 25% of the nearly 690,000 ischemic strokes each year in the United States.<sup>1</sup> Nationally, over a recent 4-year period, 491,944 carotid endarterectomies (CEAs) and 45,208 carotid artery stents were performed for asymptomatic disease, attempting to reduce the incidence of stroke.<sup>2</sup> Treatment decisions are still predominantly based upon studies correlating the risk reduction obtained from operation with percent carotid stenosis. The Asymptomatic Carotid Artery Study, Asymptomatic Carotid Surgery Trial, and other studies have reported a risk reduction with surgery for asymptomatic patients with >50% to 60% stenosis.<sup>3-7</sup> However, current risk stratification based on percent stenosis does not provide patient-specific information on the actual risk of stroke for most individuals with carotid disease. It is not surprising that prospective randomized studies have found that only 10%–12% of these asymptomatic patients will have a symptomatic stroke within 5 years, and the significant majority will never have a cerebrovascular event.<sup>3-5,7</sup> For asymptomatic patients, 19 procedures are needed to prevent one stroke.<sup>4</sup>

Most importantly, percent stenosis measurements may be a poor indicator of plaque composition and instability. Recent

reports have concluded that cerebral ischemic events associated with carotid plaque appear to be intimately associated with plaque instability.<sup>8-20</sup> Histologic analysis of high-risk plaques demonstrates intraplaque hemorrhage (IPH), lipid deposition, and necrosis.<sup>21</sup> Subgroup analysis of retrospective studies has found that plaque composition is important in risk stratification.<sup>11,19,21-23</sup>

**Plaque imaging.** Carotid duplex ultrasound is the primary diagnostic modality for evaluating carotid artery disease, with computed tomography angiography (CTA) and magnetic resonance angiography (MRA) used in the setting of acute stroke work-up and digital subtraction angiography reserved for selected cases and for mechanical thrombectomy. While CTA is accurate for measuring percent stenosis and can identify ulceration, magnetic resonance imaging (MRI) has the additional ability to measure plaque components.<sup>16,17,21,23-27</sup> In this manner, MRI can provide far more detailed information than other currently available techniques.

Currently, CTA is used far more often than MRA at our institution and nationally. While CTA has higher resolution compared to MRA, both detect lumen stenosis with a similar high accuracy compared to digital subtraction angiography.<sup>28</sup> MRI has the added benefit of detecting IPH with high accuracy using heavily T1-weighted sequences.

In contrast, published reports indicate that CTA is not reliable for IPH determination using Hounsfield units.<sup>29</sup> If determining the etiology of an acute stroke requires information on carotid plaque composition, and specifically IPH, techniques providing such information may be a requisite part of clinical evaluation.

**Importance of IPH.** The importance of carotid IPH in identifying patients at risk for stroke has been reported in multiple studies using various combinations of MRI sequences.<sup>10,13,15–18,23,30–35</sup> Lusby and colleagues first reported in 1982 that IPH is a marker for a symptomatic carotid plaque. Their retrospective study found IPH in a significantly higher proportion of CEA specimens from symptomatic as opposed to asymptomatic individuals.<sup>9</sup> IPH has been linked to increases in both necrotic core size and plaque volume.<sup>18</sup> Microscopic examination of endarterectomy specimens often demonstrates a series of microhemorrhages in the necrotic core.<sup>36</sup> These microhemorrhages lead to further plaque growth and instability.<sup>37</sup> Further, patients with baseline IPH are at significantly higher risk of further hemorrhage.<sup>31</sup> Heterogeneous plaques with IPH have been correlated with a higher incidence of prior embolic stroke.<sup>13,16,17,21,31</sup> Ouhous identified an increased number of white matter lesions in patients where the carotid bifurcation had IPH.<sup>14</sup> Altaf found increased risk of recurrent ipsilateral carotid symptoms in patients with IPH scheduled for CEA compared to patients without IPH as measured by direct thrombus imaging and that IPH predicts embolization during CEA as documented by MRI.<sup>11,22</sup> In comparing stroke-related symptoms with properties of excised plaque, thrombotically active plaque with IPH was associated strongly with symptomatic patients (71%) and weakly with asymptomatic patients (12%).<sup>19</sup>

IPH occurs in approximately 30%–36% of asymptomatic carotid lesions with at least 50% stenosis.<sup>8,18</sup> Retrospective studies have confirmed that IPH is associated with subsequent neurologic symptoms. A report on 75 men with asymptomatic carotid stenosis found that MRI-depicted IPH was associated

with an increased incidence of cerebrovascular events (stroke and TIA) with a hazard ratio of 3.6 and a negative predictive value (NPV) of 100%.<sup>18</sup> A study from the University of Washington of 154 patients reported a hazard ratio of 5.2 for stroke in patients with IPH relative to those without.<sup>38</sup> A report from the University of Virginia reported an odds ratio of 11.66 for stroke between patients with and without complex hemorrhagic atherosclerotic plaques.<sup>21</sup> Recent reports have concluded that IPH plays a greater role in plaque destabilization than was previously thought.<sup>16,31,39–41</sup>

Further, retrospective reviews have reported that the NPV of IPH in predicting ipsilateral stroke is between 92% and 100%.<sup>11,18,22</sup> This NPV clearly indicates that patients without IPH are at much lower risk of events than suggested by natural history studies on patients with moderate to severe carotid stenosis.<sup>23</sup> Figure 1 was constructed to show the significant potential of IPH to stratify the stroke risk of patients with at least 50% carotid stenosis.

As can be seen in Figure 1, retrospective findings suggest that approximately 18% of patients with IPH will have symptomatic cerebral infarction and 43% will have either a symptomatic or asymptomatic cerebral infarction within 48 months. In contrast, only 3% of patients without IPH will have a symptomatic stroke and 8% will have an asymptomatic infarct during the same time period.<sup>4,18,21,38,42–44</sup> IPH presence, volume, continuity with the lumen, and continuity with ulceration have been found to be most predictive in published retrospective reports.<sup>15–17,27,39,45–47</sup> A retrospective review found that, compared with asymptomatic patients, symptomatic patients had a higher incidence of IPH, volume ( $P = 0.003$ ), presence of juxtaluminal hemorrhage or thrombus ( $P = 0.039$ ), and lumen area reduction with ulceration ( $P = 0.008$ ).<sup>38</sup> To validate these projections and determine the relationship between IPH identified by the magnetization prepared rapid acquisition gradient echo (MPRAGE) sequence in carotid plaque and contemporary

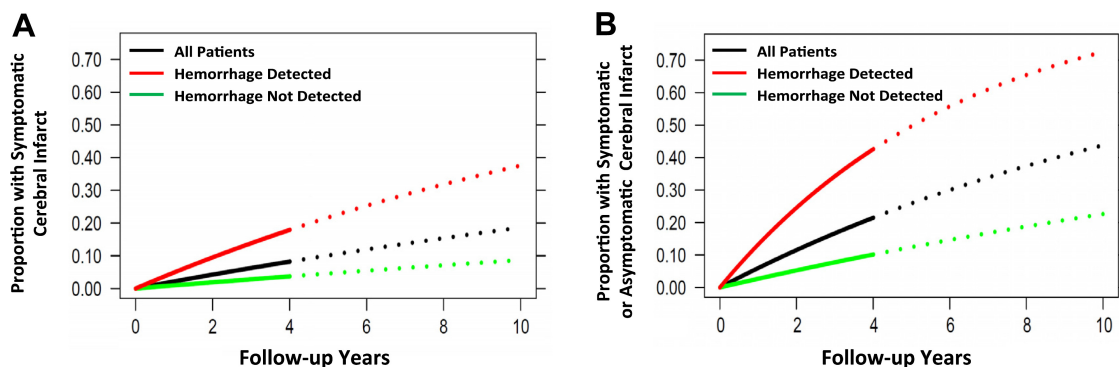


**Figure 1.** Shown are the projected cumulative probabilities of occurrence of symptomatic cerebral infarct (Panel A) and of either symptomatic or asymptomatic cerebral infarct (Panel B) for the full population (black), patients with IPH (red), and patients without IPH (green) under the reported hazard ratio of 5.2<sup>31</sup> for stroke based on presence of hemorrhage on MRI. The curves were constructed for patients with 50% stenosis assuming an overall annual 2.2% rate of symptomatic cerebral infarct,<sup>4,7,61</sup> a 4.0% rate of silent cerebral infarction,<sup>43–45</sup> and a competing risk of nonstroke death with a rate of 1.225% per year.

cerebrovascular events, we have undertaken several studies to better identify the ability of MRI to accurately detect IPH and better determine its role in stroke.

## Methods

**Patient population.** To determine the importance of IPH in acute stroke, Institutional Review Board (IRB) approval was obtained for a cross-sectional study on patients undergoing stroke evaluation within 1 week of symptom onset with brain MRI/carotid MRA with the MPRAGE sequence at the University of Utah Medical Center from November 2009 to January 2014.<sup>48–50</sup> This research was conducted in accordance with the principles of the Declaration of Helsinki. During this time, 578 patients underwent brain MRI/carotid MRA, resulting in 1,156 carotid artery–ipsilateral brain image pairs. Of these, 420 carotid brain pairs were excluded for lesions outside of 2 cm above and below the carotid bifurcation, craniocervical dissections (118), atrial fibrillation (94), intracardiac/extracardiac shunt (86), cardiac thrombus (26), recent aortic or mitral valve replacement (16), vasculitis (14), global hypoxic/ischemic injury (10), recent cardiac or neurovascular catheterization (10), recent cardiovascular surgery (8), dural venous sinus thrombosis (8), fibromuscular dysplasia or lupus vasculopathy (8), proximal common carotid stenosis  $\geq 50\%$  (6), rheumatic heart disease (4), brain neoplasm (4), endocarditis (2), idiopathic hypertrophic subaortic stenosis (2), aortic graft complication (2), and distal vessel atherosclerosis (2). Occluded carotid arteries (7) and extremely high grade lesions (3) were excluded as well, providing 726 carotid plaques for the final analysis.

**MRI/MRA protocol.** Images were obtained on Siemens 3 T and 1.5 T MRI scanners with standard head/neck coils. Standard clinical MRI/MRA protocol included brain MRI [axial diffusion-weighted images (DWI), axial T2w, axial fluid attenuation inversion recovery (FLAIR), and sagittal T1w images], brain MRA (3-D axial time of flight (TOF)), and neck MRA (2D axial TOF, coronal precontrast T1w, coronal postcontrast arterial and venous phase images). Neck MRA was obtained from the aortic arch through the circle of Willis. The total scan time was ~45 minutes, of which MPRAGE required ~5 minutes. In cases when renal insufficiency precluded intravenous contrast [glomerular filtration rate (GFR)  $< 30$  mL/min/1.73 m<sup>2</sup>], post-contrast MRA images were replaced with 3-D noncontrast (TOF) with 1-mm slice thickness combined with duplex ultrasound.

**Carotid MPRAGE sequence.** The MPRAGE sequence was used to detect IPH, and is shown in Figure 2. The parameters were first optimized at 3 T and then transferred to 1.5 T, and were as follows: 3-D, repetition time (TR)/echo time (TE)/time to inversion (TI) = 6.39/2.37/370 ms, flip angle = 15°, field of view (FOV) = 130 × 130 × 48 mm<sup>3</sup>, matrix = 256 × 256 × 48, voxel = 0.5 × 0.5 × 1.0 mm<sup>3</sup>, fat saturation, and acquisition time ~5 minutes. An initial TI of ~500 ms was chosen based on prior computer simulations at 3 T and was adjusted down to a TI of 370 ms to maximize the contrast between hemorrhage and inflowing blood in volunteer subjects, as described previously.<sup>47,51</sup> Images were obtained from 2 cm below to 2 cm above the carotid bifurcation at 1.0 mm slice thickness.

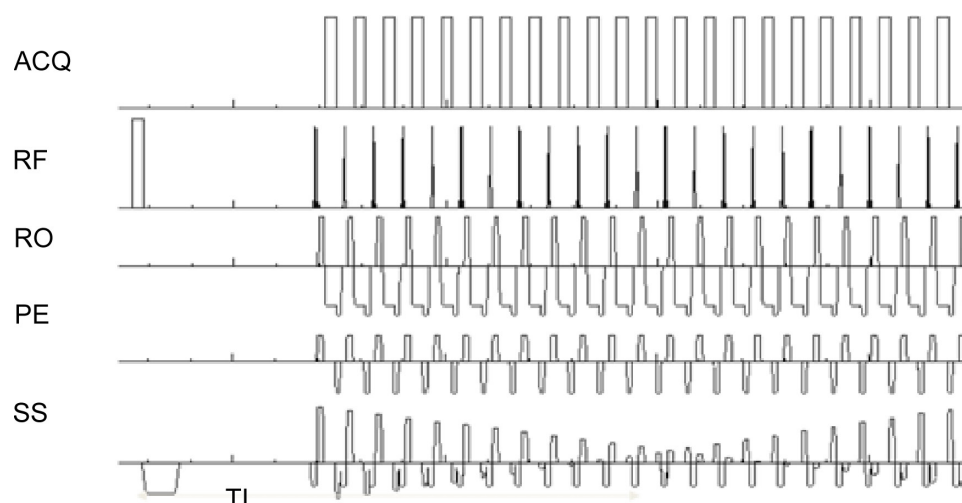


**Figure 2.** Modified 3-D MPRAGE sequence. Three-dimensional (3-D) pulse sequence diagram, modified from the Siemens MPRAGE pulse sequence (0.5 × 0.5 × 1.0 mm<sup>3</sup>, TI = 370 ms, TR = 670 ms, 48 slice locations, two averages, scan time 5 minutes 30 seconds). We have found that these modifications clearly identify recent hemorrhage as a hyperintense signal. From top to bottom, ACQ = acquisition, RF = radio frequency, RO = readout, PE = phase encoding, SS = slice select gradient. Chemical fat saturation is used. In order to produce 3-D images, a secondary phase encoding occurs in the slice select direction. One of the main advantages of our sequence is that an initial non-slice-selective 180° RF pulse is used to invert all tissues. Following the 180° RF pulse, T1 recovery during the TI interval is used to maximize the contrast between blood and tissue (T1 hemorrhage ~500 ms). Heavily T1-weighted hematoma remains hyperintense. Image acquisition time with each sequence is under 5 minutes.



**Carotid MPRAGE interpretation.** MPRAGE positive plaque was defined by at least 1 voxel with at least twofold higher signal intensity relative to adjacent sternocleidomastoid muscle.<sup>32</sup> MPRAGE status was determined independently by two radiologists blinded to patient characteristics, histology results, and adjacent images. In the 12 patients undergoing CEA, the radiologists outlined the areas of MPRAGE-positive plaque on 100 images to compare with areas of IPH and lipid/necrosis as defined by histology. Other carotid lumen markers were determined as previously described.<sup>48</sup>

**Histology validation of the MPRAGE sequence.** After informed consent, 12 patients were recruited for an IRB-approved histologic study on patients undergoing CEA.<sup>49</sup> In this subset, we determined the ability of carotid MPRAGE to detect IPH. Each carotid plaque specimen was fixed in 10% neutral buffered formalin for 3 days in preparation for histology. The ratio of fixative to specimen was at least 10:1. Specimens were decalcified in 1% Enhanced Decalcification Formulation™. The sections were submitted sequentially from inferior to superior in plastic tissue cassettes. Tissue cassettes were processed on an automated Sakura vacuum infiltrating processor, embedded in paraffin wax, sectioned at 3–4 mm intervals, and stained with hematoxylin and eosin (H&E) and Mallory's phosphotungstic acid hematoxylin (PTAH) for fibrin. A total of 100 carotid MPRAGE image/histology pairs were obtained from the 12 subjects.

**Histology interpretation of IPH.** A pathologist outlined recent IPH and lipid/necrosis using H&E and PTAH stains, blinded to MPRAGE results. "Recent" or subacute IPH was defined by one of the following: intact red blood cells, or degenerated red blood cells on H&E with PTAH stain positive for fibrin. Prior research has demonstrated that fibrin corresponds to recent IPH, within 6 weeks of age.<sup>52</sup> Lipid/necrosis was detected on H&E stain and defined as any of the following: extracellular lipid droplet accumulation, cholesterol clefts, or acellular granular debris (necrosis). Chronic hemorrhage was not detected using this T1-weighted sequence and not considered in the analysis. Carotid bifurcation and gross morphology were used as anatomic guides to pair each MPRAGE slice with the corresponding histology slide. Each carotid MPRAGE positive area was then compared with (1) IPH area, (2) lipid/necrosis area overlapping with IPH, (3) lipid/necrosis area without IPH, and (4) total plaque area.

**Inter and Intraobserver variability and 3 T versus 1.5 T substudy.** Inter and intraobserver variability was determined in a substudy of 362 patients undergoing carotid MRI from 2009 to 2011.<sup>49</sup> Images were obtained using the 3-D MPRAGE sequence on Siemens 3 T and 1.5 T MRI scanners. At 1.5 T, 282 patients were scanned, yielding 564 carotids, 2 of which were occluded. At 3 T, 32 patients (64 carotids) underwent MRI with standard coils, and 48 patients (90 carotids, 6 occluded) underwent MRI using custom-made bilateral dual-element phased array coils.<sup>51</sup> There was no significant difference in image quality at 3 T with standard coils versus custom coils

( $3.84 \pm 0.09$  vs  $3.89 \pm 0.09$ ,  $\pm$  SEM,  $P = 0.70$ ). At 1.5 T, all carotid MPRAGE images were obtained with standard neck coils. MPRAGE status was determined in each complete arterial segment in patients undergoing carotid MPRAGE at 3 T versus 1.5 T. Interobserver agreement was determined between observers 1 and 2. Intraobserver agreement was determined for observer 1.

**Acute stroke determination.** Recent carotid territory infarct was defined as either clinically symptomatic or asymptomatic acute infarct in the ipsilateral territory of the ICA confirmed by DWI technique derived from DTI trace images from our standard clinical imaging protocol, as previously described.<sup>50</sup> DTI trace images have been shown to be superior to conventional diffusion-weighted sequences in detecting recent infarcts.<sup>53</sup>

**Statistical analysis.** To determine the optimal prediction of carotid-source stroke, a mixed-effects multivariable Poisson regression model was used accounting for two vessels per patient. The Poisson regression model was fitted for the outcome of carotid IPH with carotid imaging predictors including percent diameter stenosis, mm stenosis, maximum plaque thickness, ulceration, and intraluminal thrombus. Clinical covariates included age, male sex, diabetes, hypertension, hyperlipidemia, and body mass index. Cardiovascular medication confounders included antihypertension, antiplatelet, anticoagulation, and statin medication classes. In addition, magnet strength (3 T or 1.5 T) was included as a potential confounder in the Poisson regression model. A backward-elimination method was used to determine the final model, in which all remaining predictors had a  $P < 0.10$ . Prevalence ratios and  $P$ -values were reported for each factor alone and for the factors found to be significant from the backward elimination. Similarly, mixed-effects multivariable Poisson regression was used to determine essential imaging and clinical predictors of carotid IPH.

In the histology substudy, we compared MPRAGE-positive area to histology-defined hemorrhage and lipid/necrosis areas (all measured as mm<sup>2</sup>). We used a random-intercept linear regression model with an autoregressive correlation structure. In this repeated measures analysis of the 12 CEA subjects, the "time" repetition variable was the slice position as measured in millimeters relative to the bifurcation. Using MPRAGE area as the outcome variable, our predictor variables were analyzed one at a time and included 1) IPH area (with or without lipid/necrosis), 2) lipid/necrosis area overlapping with IPH, 3) lipid/necrosis area without IPH, and 4) total plaque area. In the final model, all of the above predictor variables were included. Kappa analysis was used to calculate inter- and intraobserver agreement. All statistical analyses were performed with Stata version 13.1.

## Results

**Patient demographics.** Patient demographics are listed by vessel below in Table 1.

**MPRAGE signal predicts histology-defined carotid IPH.** One hundred carotid MPRAGE image/histology pairs

**Table 1.** Patient demographics.

Demographics by vessel (total n = 726)	
Stroke, no. (%)	100 (13.8)
Male sex, no. (%)	387 (53.3)
Age, mean (SD) (years)	64.2 (15.6)
Body mass index (BMI), mean (SD) (kg/m <sup>2</sup> )	28.4 (6.4)
Smoking, no. (%)	
Current smoker	138 (19.0)
Prior smoker	158 (21.8)
Never smoker	430 (59.2)
Hypertension, no. (%)	499 (68.7)
Hyperlipidemia, no. (%)	358 (49.3)
Diabetes, no. (%)	227 (31.3)
Cardiovascular medications	
Antihypertension, no. (%)	412 (56.8)
Statin, no. (%)	316 (43.5)
Antiplatelet, no. (%)	294 (40.5)
Anticoagulation, no. (%)	74 (10.2)
Carotid plaque imaging markers	
Stenosis, mean (SD), %	12.2 (23.1)
Mild stenosis (0–49%), no. (%)	647 (89.1)
Moderate stenosis (50%–69%), no. (%)	45 (6.2)
Severe stenosis (70%–99%), no. (%)	34 (4.7)
Stenosis, mean (SD) (mm)	4.1 (1.2)
Maximum plaque thickness, mean (SD) (mm)	3.0 (1.6)
Ulceration, no. (%)	96 (13.2)
Intraluminal thrombus, no. (%)	19 (2.6)
Intraplaque hemorrhage, no. (%)	65 (9.0)
Magnet strength = 3 T, no. (%)	58 (8.0)

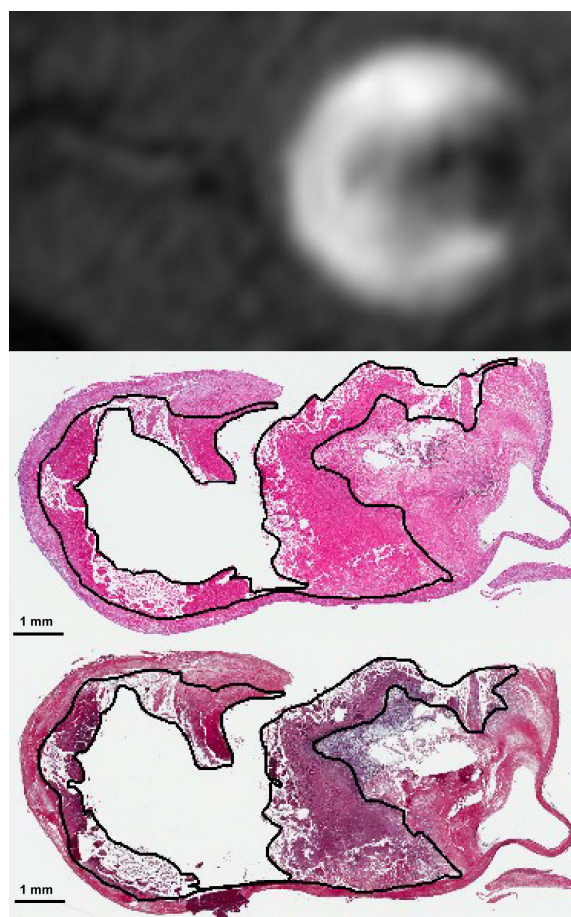


**Figure 3.** Comparison of carotid MPRAGE and IPH detected on histology. Top: Representative MPRAGE positive plaque in a patient undergoing subsequent endarterectomy. Middle: H&E stain demonstrating recent IPH (solid line) outlined by a pathologist. Bottom: PTAH positive staining (solid line) also indicates fibrin deposition and recent IPH.

from 12 patients who underwent surgery were analyzed using a linear mixed model. Histology-defined area of IPH significantly predicted MPRAGE-positive area (slope = 0.52,  $P < 0.001$ , 95% CI: 0.41, 0.64, see representative image demonstrating IPH detection with MPRAGE in Fig. 3). Lipid/necrosis without IPH was not a significant predictor of the MPRAGE-positive area (slope = 0.01,  $P = 0.846$ , 95% CI: -0.13, 0.16). Total plaque area was a significant predictor of MPRAGE-positive area (slope = 0.20,  $P < 0.001$ , 95% CI: 0.10, 0.30). Kappa values for inter- and intraobserver agreement on MPRAGE hyperintensity in this segment of the study were 0.818 and 0.806, respectively, indicating very good agreement.

**Carotid MPRAGE inter- and intraobserver agreement.** Overall, the Kappa value for interobserver agreement was 0.812. After adjusting for prevalence and bias, the overall PABAK for interobserver agreement was 0.944. The Kappa value for interobserver agreement was 0.807 at 3 T and 0.803 at 1.5 T. After adjusting for prevalence and bias, the

PABAK was 0.883 at 3 T and 0.961 at 1.5 T. The intraobserver agreement of carotid MPRAGE was determined at 3 T versus 1.5 T for observer 1 with pooled data and Kappa and PABAK. Overall, the Kappa value for intraobserver agreement was 0.899.

**Carotid-source stroke prediction using multivariable Poisson regression.** Representative images demonstrating carotid IPH prediction of ipsilateral stroke are shown in Figure 4. After backward elimination with a threshold of  $P < 0.10$ , the significant factors predicting carotid-source stroke included IPH (prevalence ratio, PR = 5.61,  $P < 0.001$ , 95% confidence interval (CI) = 3.77, 8.35), intraluminal thrombus (PR 3.60,  $P < 0.001$ , 95% CI = 2.23, 5.81), current smoking (PR = 1.77,  $P = 0.007$ , 95% CI = 1.17, 2.68), and maximum thickness (PR = 1.13,  $P = 0.005$ , 95% CI = 1.04, 1.24). Prior smoking was not a significant predictor of carotid-source stroke (PR = 1.35,  $P = 0.121$ , 95% CI = 0.92, 1.96), but was included in the final model since current smoking was significant.

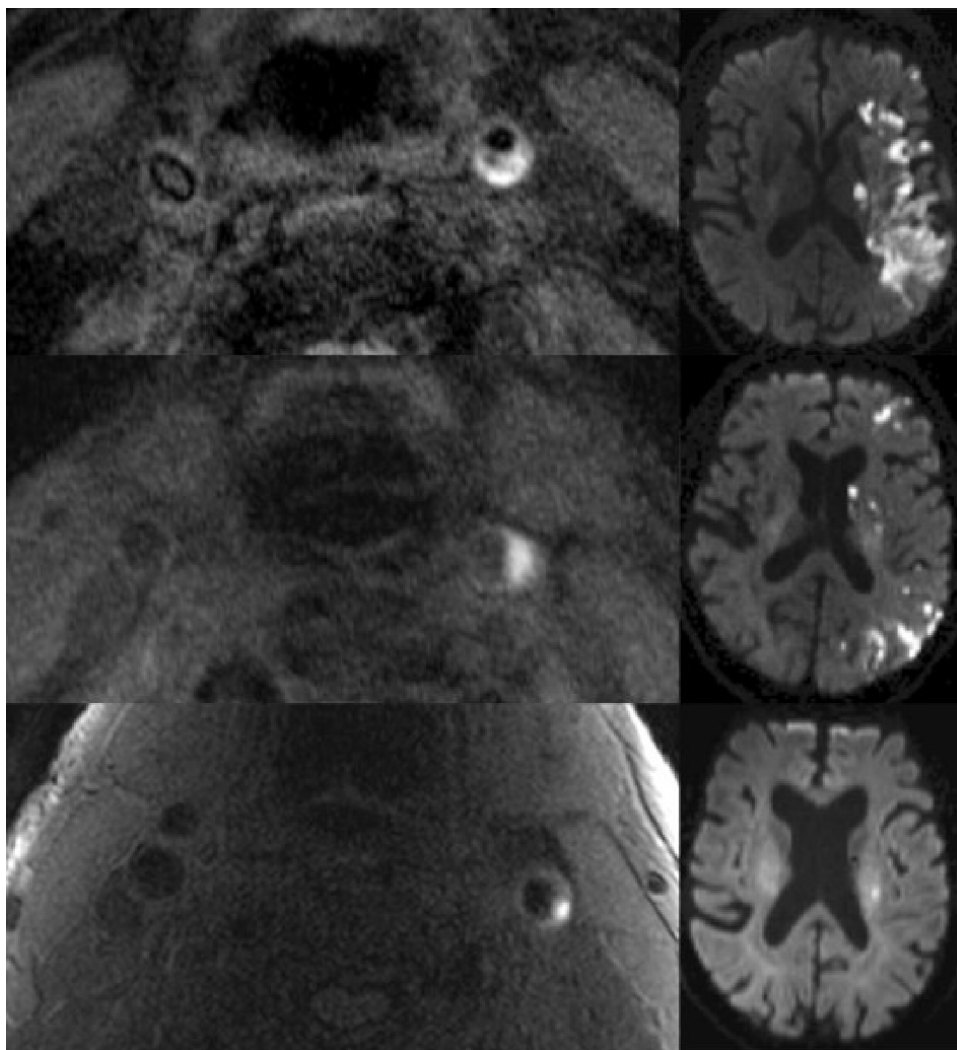


**Figure 4.** Left: MPRAGE hyperintense signal demonstrating IPH in ICA plaque in the three separate patients. From top to bottom: large, moderate and small IPH is present in the left ICA. Right: Corresponding DWI images showing infarction in each patient’s IPH positive left ICA distribution.

**Carotid IPH prediction using multivariable Poisson regression.** After backward-elimination with a threshold of  $P < 0.10$ , the remaining significant factors predicting carotid IPH included maximum plaque thickness (PR = 1.34,  $P < 0.001$ , 95% CI = 1.21, 1.48), mm stenosis (PR = 0.71,  $P < 0.001$ , 95% CI = 0.61, 0.85), ulceration (PR = 1.83,  $P = 0.011$ , 95% CI = 1.15, 2.92), age (PR = 1.04,  $P < 0.001$ , 95% CI = 1.03, 1.06), and male sex (PR = 1.83,  $P = 0.079$ , 95% CI = 0.93, 3.59).

**Summary and pathway analysis.** Pathway analysis demonstrating predictors of carotid IPH (stenosis, ulceration, age, male sex, and plaque thickness) and predictors of carotid-source stroke (carotid IPH, intraluminal thrombus, plaque thickness, and current smoking) is presented in Figure 5.

**Discussion**

Determining stroke etiology is critically important, since surgery has proven very effective in preventing strokes from carotid artery lesions. IPH has a strong correlation with acute strokes,

and this relationship remains highly significant even when considering the effect of other available lumen markers (stenosis, thickness, ulceration, and intraluminal thrombus). These results suggest that IPH identified on carotid MRI can significantly improve our ability to identify strokes from carotid disease and identify individuals likely to benefit from intervention.

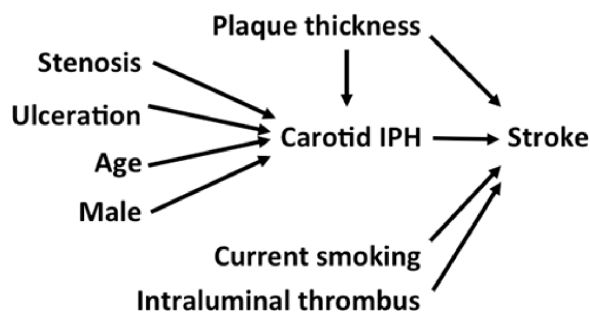


**Figure 5.** Pathway analysis demonstrating predictors of carotid IPH and carotid-source stroke.



Since this report is not based upon longitudinal MRI imaging of IPH, we cannot determine the natural evolution of IPH over time. However, other studies have found that IPH is a marker of stroke risk, conferring a stroke risk over up to 5 years. These longitudinal studies from the University of Washington indicate that many features of IPH are stable over time. While methemoglobin does not persist indefinitely, it appears that there may be ongoing low-level plaque hemorrhage that continues to produce the methemoglobin over time. This could account for methemoglobin being identified on serial exams in many but not all patients.

Ensuring accurate and reproducible IPH identification is critical. In our prior research, we determined that MPRAGE-positive signal detects IPH but not lipid/necrosis. In addition, we found that the carotid MPRAGE detection of IPH has high inter- and intraobserver agreement at both 1.5 T and 3 T.

Carotid IPH is generally differentiated from carotid dissection by its location. IPH is associated with atherosclerotic risk factors and is found where carotid plaque is found. As opposed to dissection, IPH is centered at the carotid bifurcation with a predilection to the outer wall opposite the flow divider because of the oscillatory shear stress in this location. In contrast, dissection begins in the cervical ICA superior to the bifurcation and extends to the intracerebral ICA above the angle of the mandible. Dissection occurs in younger individuals without atherosclerotic risk factors, and does not primarily involve the outer wall of the bifurcation.

Our data would suggest that stroke risk is independent of the size of IPH, but we do not have quantifiable data on subjects in our larger longitudinal studies to confirm this clinical impression. While consideration of both intraluminal thrombus and IPH improves the correlation of carotid disease with acute stroke in our experience, IPH added no further discriminatory value in the relatively rare instance of intraluminal thrombus detection. These findings are not intuitive, since stroke from carotid atherosclerosis has always been thought to occur from initial thrombus formation and subsequent fragmentation and embolization. While thrombi likely also form with IPH, these may be below the limits of detection or they may have already undergone cerebral embolization. Confirmation of IPH-induced microthrombi could be obtained with future studies using high-resolution methods including optical coherence tomography (OCT).<sup>54</sup>

The explanation for the increased stroke risk with IPH may be multifactorial. IPH is thought to result from plaque microvessel leakage, and may be a marker of an inflamed plaque with endothelial dysfunction. IPH may also directly contribute to plaque inflammation through iron deposition and reactive oxygen species formation.<sup>55</sup> In addition, IPH has been shown to rapidly increase plaque size and stenosis.<sup>56</sup> This can result in pathologic changes in endothelial mechanotransduction related to oscillatory shear stress, resulting in endothelial oxidative stress and inflammation and contributing to stroke risk.<sup>57</sup>

While these data are somewhat limited due to their cross-sectional nature, they nonetheless argue against using only stenosis to determine carotid stroke sources.

## Conclusion

The presence of IPH can be accurately determined with heavily T1-weighted MRI sequences and strongly predicts stroke. Intervention based upon carotid stenosis alone results in the vast majority of procedures being performed on individuals who will never have a stroke. With advances in imaging, evidence supporting stroke risk stratification based on IPH is rapidly accumulating.<sup>58–60</sup> Intervention based upon the presence of IPH has the potential, if validated by other prospective longitudinal studies, to dramatically reduce the number of carotid interventions, reducing the number of operative strokes and deaths while savings significant medical resources. It will also improve selection of those individuals who are at higher risk of neurologic events and may truly benefit from intervention. While optimal discrimination of carotid-source stroke may require information on IPH, intraluminal thrombus, other plaque characteristics, and clinical information, IPH alone is strongly predictive of subsequent stroke risk and should be considered as the basis for surgical intervention.

## Author Contributions

Conceived and designed the experiments: GST, JSM, SEK, DLP. Analyzed the data: GST, JSM, DLP. Wrote the first draft of the manuscript: GST. Contributed to the writing of the manuscript: GST, JSM, SEK, DLP. Agree with manuscript results and conclusions: GST, JSM, SEK, DLP. Jointly developed the structure and arguments for the paper: GST, JSM. Made critical revisions and approved final version: GST, JSM, SEK, DLP. All authors reviewed and approved of the final manuscript.

## REFERENCES

1. Lloyd-Jones D, Adams RJ, Brown TM, et al. Heart disease and stroke statistics—2010 update: a report from the American Heart Association. *Circulation*. 2010; 121(7):e46–e215.
2. McPhee JT, Schanzer A, Messina LM, Eslami MH. Carotid artery stenting has increased rates of postprocedure stroke, death, and resource utilization than does carotid endarterectomy in the United States, 2005. *J Vasc Surg*. 2008;48(6):1442–1450. 1450 e1441.
3. Carotid surgery versus medical therapy in asymptomatic carotid stenosis. The CASANOVA Study Group. *Stroke*. 1991;22(10):1229–1235.
4. Endarterectomy for asymptomatic carotid artery stenosis. Executive Committee for the Asymptomatic Carotid Atherosclerosis Study. *JAMA*. 1995;273(18): 1421–1428.
5. Risk of stroke in the distribution of an asymptomatic carotid artery. The European Carotid Surgery Trialists Collaborative Group. *Lancet*. 1995;345(8944):209–212.
6. Mackey AE, Abrahamowicz M, Langlois Y, et al. Outcome of asymptomatic patients with carotid disease. Asymptomatic Cervical Bruit Study Group. *Neurology*. 1997;48(4):896–903.
7. Halliday A, Mansfield A, Marro J, et al. Prevention of disabling and fatal strokes by successful carotid endarterectomy in patients without recent neurological symptoms: randomised controlled trial. *Lancet*. 2004;363(9420):1491–1502.
8. Lovett JK, Gallagher PJ, Hands LJ, Walton J, Rothwell PM. Histological correlates of carotid plaque surface morphology on lumen contrast imaging. *Circulation*. 2004;110(15):2190–2197.
9. Lusby RJ, Ferrell LD, Ehrenfeld WK, Stoney RJ, Wylie EJ. Carotid plaque hemorrhage. Its role in production of cerebral ischemia. *Arch Surg*. 1982;117(11):1479–1488.



10. Moody AR, Murphy RE, Morgan PS, et al. Characterization of complicated carotid plaque with magnetic resonance direct thrombus imaging in patients with cerebral ischemia. *Circulation*. 2003;107(24):3047–3052.
11. Altaf N, Beech A, Goode SD, et al. Carotid intraplaque hemorrhage detected by magnetic resonance imaging predicts embolization during carotid endarterectomy. *J Vasc Surg*. 2007;46(1):31–36.
12. Chu B, Kampschulte A, Ferguson MS, et al. Hemorrhage in the atherosclerotic carotid plaque: a high-resolution MRI study. *Stroke*. 2004;35(5):1079–1084.
13. Li ZY, Howarth SP, Tang T, et al. Structural analysis and magnetic resonance imaging predict plaque vulnerability: a study comparing symptomatic and asymptomatic individuals. *J Vasc Surg*. 2007;45(4):768–775.
14. Ouhlous M, Flach HZ, de Weert TT, et al. Carotid plaque composition and cerebral infarction: MR imaging study. *AJNR Am J Neuroradiol*. 2005;26(5):1044–1049.
15. Raman SV, Winner MW III, Tran T, et al. In vivo atherosclerotic plaque characterization using magnetic susceptibility distinguishes symptom-producing plaques. *JACC Cardiovasc Imaging*. 2008;1(1):49–57.
16. Saam T, Hatsukami TS, Takaya N, et al. The vulnerable, or high-risk, atherosclerotic plaque: noninvasive MR imaging for characterization and assessment. *Radiology*. 2007;244(1):64–77.
17. Sharma R. MR imaging in carotid artery atherosclerosis plaque characterization. *Magn Reson Med Sci*. 2002;1(4):217–232.
18. Singh N, Moody AR, Gladstone DJ, et al. Moderate carotid artery stenosis: MR imaging-depicted intraplaque hemorrhage predicts risk of cerebrovascular ischemic events in asymptomatic men. *Radiology*. 2009;252(2):502–508.
19. Spagnoli LG, Mauriello A, Sangiorgi G, et al. Extracranial thrombotically active carotid plaque as a risk factor for ischemic stroke. *JAMA*. 2004;292(15):1845–1852.
20. Wallis de vries BM, van Dam GM, Tio RA, Hillebrands JL, Slart RH, Zeebregts CJ. Current imaging modalities to visualize vulnerability within the atherosclerotic carotid plaque. *J Vasc Surg*. 2008;48(6):1620–1629.
21. Parmar JP, Rogers WJ, Mugler JP III, et al. Magnetic resonance imaging of carotid atherosclerotic plaque in clinically suspected acute transient ischemic attack and acute ischemic stroke. *Circulation*. 2010;122(20):2031–2038.
22. Altaf N, MacSweeney ST, Gladman J, Auer DP. Carotid intraplaque hemorrhage predicts recurrent symptoms in patients with high-grade carotid stenosis. *Stroke*. 2007;38(5):1633–1635.
23. Saam T, Cai J, Ma L, et al. Comparison of symptomatic and asymptomatic atherosclerotic carotid plaque features with in vivo MR imaging. *Radiology*. 2006;240(2):464–472.
24. Clarke SE, Hammond RR, Mitchell JR, Rutt BK. Quantitative assessment of carotid plaque composition using multicontrast MRI and registered histology. *Magn Reson Med*. 2003;50(6):1199–1208.
25. Golledge J, Greenhalgh RM, Davies AH. The symptomatic carotid plaque. *Stroke*. 2000;31(3):774–781.
26. Hatsukami TS, Ross R, Polissar NL, Yuan C. Visualization of fibrous cap thickness and rupture in human atherosclerotic carotid plaque in vivo with high-resolution magnetic resonance imaging. *Circulation*. 2000;102(9):959–964.
27. Saam T, Ferguson MS, Yarnykh VL, et al. Quantitative evaluation of carotid plaque composition by in vivo MRI. *Arterioscler Thromb Vasc Biol*. 2005;25(1):234–239.
28. Anzidei M, Napoli A, Zaccagna F, et al. Diagnostic accuracy of colour Doppler ultrasonography, CT angiography and blood-pool-enhanced MR angiography in assessing carotid stenosis: a comparative study with DSA in 170 patients. *Radiol Med*. 2012;117(1):54–71.
29. JMUK-I, Fox AJ, Aviv RL, et al. Characterization of carotid plaque hemorrhage: a CT angiography and MR intraplaque hemorrhage study. *Stroke*. 2010;41(8):1623–1629.
30. Mofidi R, Crotty TB, McCarthy P, Sheehan SJ, Mehigan D, Keaveny TV. Association between plaque instability, angiogenesis and symptomatic carotid occlusive disease. *Br J Surg*. 2001;88(7):945–950.
31. Takaya N, Yuan C, Chu B, et al. Presence of intraplaque hemorrhage stimulates progression of carotid atherosclerotic plaques: a high-resolution magnetic resonance imaging study. *Circulation*. 2005;111(21):2768–2775.
32. Yamada N, Higashi M, Otsubo R, et al. Association between signal hyperintensity on T1-weighted MR imaging of carotid plaques and ipsilateral ischemic events. *AJNR Am J Neuroradiol*. 2007;28(2):287–292.
33. Hishikawa T, Iihara K, Yamada N, Ishibashi-Ueda H, Miyamoto S. Assessment of necrotic core with intraplaque hemorrhage in atherosclerotic carotid artery plaque by MR imaging with 3D gradient-echo sequence in patients with high-grade stenosis. Clinical article. *J Neurosurg*. 2010;113(4):890–896.
34. Rao DS, Goldin JG, Fishbein MC. Determinants of plaque instability in atherosclerotic vascular disease. *Cardiovasc Pathol*. 2005;14(6):285–293.
35. Murphy RE, Moody AR, Morgan PS, et al. Prevalence of complicated carotid atheroma as detected by magnetic resonance direct thrombus imaging in patients with suspected carotid artery stenosis and previous acute cerebral ischemia. *Circulation*. 2003;107(24):3053–3058.
36. Burke AP, Kolodgie FD, Farb A, et al. Healed plaque ruptures and sudden coronary death: evidence that subclinical rupture has a role in plaque progression. *Circulation*. 2001;103(7):934–940.
37. Fryer JA, Myers PC, Appleberg M. Carotid intraplaque hemorrhage: the significance of neovascularity. *J Vasc Surg*. 1987;6(4):341–349.
38. Takaya N, Yuan C, Chu B, et al. Association between carotid plaque characteristics and subsequent ischemic cerebrovascular events: a prospective assessment with MRI—initial results. *Stroke*. 2006;37(3):818–823.
39. Saam T, Yuan C, Chu B, et al. Predictors of carotid atherosclerotic plaque progression as measured by noninvasive magnetic resonance imaging. *Atherosclerosis*. 2007;194(2):e34–e42.
40. Kolodgie FD, Gold HK, Burke AP, et al. Intraplaque hemorrhage and progression of coronary atheroma. *N Engl J Med*. 2003;349(24):2316–2325.
41. Virmani R, Kolodgie FD, Burke AP, et al. Atherosclerotic plaque progression and vulnerability to rupture: angiogenesis as a source of intraplaque hemorrhage. *Arterioscler Thromb Vasc Biol*. 2005;25(10):2054–2061.
42. Das RR, Seshadri S, Beiser AS, et al. Prevalence and correlates of silent cerebral infarcts in the Framingham offspring study. *Stroke*. 2008;39(11):2929–2935.
43. Romero JR, Beiser A, Seshadri S, et al. *Silent Cerebral Infarction Exceeds that of Clinical Stroke in Mid-life: The Framingham Heart Study*. San Diego, CA: FHS; 2009:129.
44. Vermeer SE, Hollander M, van Dijk EJ, Hofman A, Koudstaal PJ, Breteler MM. Silent brain infarcts and white matter lesions increase stroke risk in the general population: the Rotterdam Scan Study. *Stroke*. 2003;34(5):1126–1129.
45. Kampschulte A, Ferguson MS, Kerwin WS, et al. Differentiation of intraplaque versus juxtalumenal hemorrhage/thrombus in advanced human carotid atherosclerotic lesions by in vivo magnetic resonance imaging. *Circulation*. 2004;110(20):3239–3244.
46. Bitar R, Moody AR, Leung G, et al. In vivo 3D high-spatial-resolution MR imaging of intraplaque hemorrhage. *Radiology*. 2008;249(1):259–267.
47. Zhu DC, Ferguson MS, DeMarco JK. An optimized 3D inversion recovery prepared fast spoiled gradient recalled sequence for carotid plaque hemorrhage imaging at 3.0 T. *Magn Reson Imaging*. 2008;26(10):1360–1366.
48. McNally JS, McLaughlin MS, Hinckley PJ, et al. Intraluminal thrombus, intraplaque hemorrhage, plaque thickness, and current smoking optimally predict carotid stroke. *Stroke*. 2015;46(1):84–90.
49. McNally JS, Yoon HC, Kim SE, et al. Carotid MRI Detection of Intraplaque Hemorrhage at 3T and 1.5T. *J Neuroimaging*. 2014. doi: 10.1111/jon.12146.
50. McNally JS, Kim SE, Yoon HC, et al. Carotid magnetization-prepared rapid acquisition with gradient-echo signal is associated with acute territorial cerebral ischemic events detected by diffusion-weighted MRI. *Circ Cardiovasc Imaging*. 2012;5(3):376–382.
51. Hadley JR, Roberts JA, Goodrich KC, Buswell HR, Parker DL. Relative RF coil performance in carotid imaging. *Magn Reson Imaging*. 2005;23(5):629–639.
52. Derksen WJ, Peeters W, van Lammeren GW, et al. Different stages of intraplaque hemorrhage are associated with different plaque phenotypes: a large histopathological study in 794 carotid and 276 femoral endarterectomy specimens. *Atherosclerosis*. 2011;218(2):369–377.
53. Chou MC, Tzeng WS, Chung HW, et al. T2-enhanced tensor diffusion trace-weighted image in the detection of hyper-acute cerebral infarction: comparison with isotropic diffusion-weighted image. *Eur J Radiol*. 2010;74(3):e89–e94.
54. Yoshimura S, Kawasaki M, Yamada K, et al. Visualization of internal carotid artery atherosclerotic plaques in symptomatic and asymptomatic patients: a comparison of optical coherence tomography and intravascular ultrasound. *AJNR Am J Neuroradiol*. 2012;33(2):308–313.
55. Vinchi F, Muckenthaler MU, Da Silva MC, Balla G, Balla J, Jeney V. Atherogenesis and iron: from epidemiology to cellular level. *Front Pharmacol*. 2014;5:94.
56. Sun J, Underhill HR, Hippe DS, Xue Y, Yuan C, Hatsukami TS. Sustained acceleration in carotid atherosclerotic plaque progression with intraplaque hemorrhage: a long-term time course study. *JACC Cardiovasc Imaging*. 2012;5(8):798–804.
57. Harrison DG, Widder J, Grumbach I, Chen W, Weber M, Searles C. Endothelial mechanotransduction, nitric oxide and vascular inflammation. *J Intern Med*. 2006;259(4):351–363.
58. Gupta A, Baradaran H, Schweitzer AD, et al. Carotid plaque MRI and stroke risk: a systematic review and meta-analysis. *Stroke*. 2013;44(11):3071–3077.
59. Hosseini AA, Kandiyil N, Macsweeney ST, Altaf N, Auer DP. Carotid plaque hemorrhage on magnetic resonance imaging strongly predicts recurrent ischemia and stroke. *Ann Neurol*. 2013;73(6):774–784.
60. Saam T, Hetterich H, Hoffmann V, et al. Meta-analysis and systematic review of the predictive value of carotid plaque hemorrhage on cerebrovascular events by magnetic resonance imaging. *J Am Coll Cardiol*. 2013;62(12):1081–1091.
61. Halm EA, Tuhim S, Wang JJ, Rockman C, Riles TS, Chassin MR. Risk factors for perioperative death and stroke after carotid endarterectomy: results of the New York carotid artery surgery study. *Stroke*. 2009;40(1):221–229.